Data Base for a Turbulent, Nonpremixed, Nonreacting Propane-Jet Flow

Robert W. Schefer

Mail Stop 9051
Combustion Research Facility
Sandia National Laboratories
Livermore, CA 94551-0969
rwsche@ca.sandia.gov

Abstract

This database is part of the International Workshop on Measurement and Computation of Turbulent Nonpremixed Flames. Detailed experimental data have been obtained and tabulated for a variable-density, nonreacting round jet of propane into coflowing air. The data set includes mean and rms fluctuations for density and propane mixture fraction, the intermittency and the third and fourth moments. Data for the probability density distributions of mixture fraction at several axial and radial locations are also provided. Velocity data includes the mean axial and radial velocity components, the rms fluctuations of each velocity component, and the correlation between axial and radial velocity. Further discussion and analysis of the data can be found in Schefer et al. 1985, 1986 and 1987; Dibble et al. 1984; Dibble et al. 1985 and 1987; Gouldin et al. 1986).

The archive of the complete experimental data set is SANDC3H8.JET. The tabulated statistical data is contained within this archive as ASCII text files.

Use of The Data

Please contact Robert Schefer at the above address if you download and use these data. This will ensure that you will be on the mailing list for updates regarding these and other relevant data.

Also please contact if any discrepancies are discovered in this data set.

Notice

Contents

1. Experimental System Description

1.1 Flow Facility

The measurements were performed in the Sandia Turbulent Diffusion Flame Facility. A complete description of the facility is given in Dibble et al. (1984 and 1987). The facility is a forced-draft vertical wind tunnel with an axisymmetric fuel jet located at the upstream end of the test section. The fully-windowed test section has a 20-cm-square cross section and is 200-cm long. The fuel nozzle has an inside diameter of 0.526 cm and an outer diameter of 0.90 cm. The fuel jet (bulk) velocity was 53 m/s (±0.1 m/s) and the coflow air velocity was 9.2 m/s (±0.1 m/s). Test section dimensions and the inlet conditions are summarized in Table 1. Velocity measurements at the test section inlet showed that the maximum velocity at the centerline of the jet exit of $u_{j,max}$=69 m/s is consistent with fully-developed, turbulent pipe flow ($u_{j,max}$ = 1.28 $u_{j,bulk}$). A thin boundary layer was also measured along the outer edge of the jet pipe with a thickness of approximately 0.3 jet diameters at the exit plane of the jet. The experimental diagnostics used in the study and the corresponding quantities measured are summarized in Table 2.

Table 1. Test Section Dimensions and Inlet Conditions.

Orientation	Vertical
Test Section	30 cm x 30 cm
Jet Tube Exit	0.52 cm (I. D.) 0.90 cm (O. D.)
Length of Fuel Jet Tube Straight Section Prior to Exit	2 m
Propane Jet Velocity	53 m/s (±0.1 m/s)
Propane Jet Temperature	294 K (±2 K)
Coflow Air Velocity	9.2 m/s (±0.1 m/s)
Coflow Air Temperature	294 K (±2 K)
Reynolds Number (based on jet exit diameter)	68,000
Coflow Air Turbulence	0.4%
Axial Pressure Gradient	6 Pa/m

Table 2. Experimental Diagnostics.

Diagnostic	Quantity Measured
CW Rayleigh Scattering	Single-Point Density and Mixture Fraction
Laser Doppler Velocimetry	Simultaneous Single-Point Axial and Radial Velocities
Raman Scattering	Single-Point Propane Concentration
Combined LDV-Raman Scattering	Simultaneous Single-Point Propane Concentration and Two-Velocity Components
One-Dimensional Rayleigh Imaging	Instantaneous Radial Profiles of Density and Mixture Fraction

1.2 Rayleigh Scattering System

Rayleigh scattering was used for single-point density and propane mixture fraction measurements (Schefer and Dibble, 1985 and 1986). The Rayleigh scattering measurements were made using a 6-watt cw argon-ion laser operating at λ=488 nm. The laser beam was focused with a 35-cm focal length lens to a 200-μm waist diameter. The measurement volume, defined by the entrance slit to the photomultiplier tube (3-mm wide, 2-mm high) and the laser beam diameter, was 1 mm in length by 0.2 mm in diameter. At each spatial location 64,000 measurements were taken at a sample rate of 16,000 samples per second. This sample rate resulted in frequency components up to 8 kHz contributing to the mean and fluctuating Rayleigh signal.

In a two-component, isothermal flow such as the nonreacting propane jet the Rayleigh signal intensity is directly related to the propane mole fraction. The derivation of gas density and mixture fraction from propane mole fraction is straightforward (Johnston, et. al 1986). The primary sources of error in the Rayleigh scattering measurements are background scattering and shot noise. The background signal was approximately 4 percent of the Rayleigh signal measured in air. Background scattering light was eliminated by subtracting its value from the measured signal. Electronic shot noise contributes to the measured concentration fluctuations. The estimated shot noise contribution was 3 percent of the total air signal. The uncertainty in the mixture fraction measurements using Rayleigh scattering was estimated from calibration data and from the scatter in measurements from several different experimental runs. The estimated uncertainty in the data is: f= $\pm$2%, f' = $\pm$3%.

In addition to single-point Rayleigh scattering measurements, the Rayleigh technique was extended to one-dimensional measurements using an optical multichannel analyzer (OMA) to obtain information on instantaneous gradients in the flowfield. This data has been published in Dibble et al. 1985 and will not be discussed further.

1.3 Laser Doppler Velocimetry

Velocity measurements were made using a two-color laser Doppler velocimetry (LDV) system (Schefer et al. 1987). The LDV system is a two-color, dual-beam, real-fringe system with a measurement volume, as defined by the image of the pinhole on the beam crossing, 0.3 mm long by 0.25 mm in diameter. Coincidence of the radial and axial velocity measurements was verified using a multichannel interface with the variable time window set at 10 μs to assure that the velocity measurement in each direction was from the same seed particle.

The velocity data are presented as mean and rms fluctuating velocity components (axial and radial velocity) and their correlation, conditional on fluid originating from the jet or the air stream. In the data analysis, it is assumed that the seed particles (0.85-μm diameter) follow the motion of the fluid and that the difference between the diffusivity of the particle and the fluid is negligible. These assumptions are valid in the limit of large Reynolds number. With these assumptions, the motion of a seed particle is identical to the motion of a fluid element and fluid originating from the jet can be distinguished from fluid originating from the coflowing air. Thus by alternately seeding only the jet and the coflowing air streams, velocity statistics conditional on the jet fluid and on the coflowing air fluid can be obtained.

At each measurement location a minimum of 3,000 velocity measurements were obtained. This was estimated to be sufficient for the first two moments of the velocity. The correlation u'v' calculated from 3,000 measurements agreed within 1 percent of the value calculated from up to 10,000 measurements. The error due to velocity-gradient broadening was estimated to be less than 0.3 percent. Since the velocity of a particle is actually measured with laser velocimetry, particle-velocity lag must also be considered. It was estimated that a 0.85-micron particle can follow the flow up to a frequency of 8 kHz with a slip velocity of 1 percent.

The primary source of error in the present flow is bias toward higher velocities due to the proportionality of the particle flux through the measurement volume to the instantaneous velocity. This form of bias may be significant when number-weighted averages are used to calculate stationary statistics. The effect of this bias was minimized by seeding both flows heavily enough to obtain high data rates and using a time-integrated averaging method to calculate the velocity statistics. Typically the data rate was maintained above 8 kHz at all measurement locations.

The long-term repeatability of the measurements was established by repeating the measurements at selected locations after the initial data set was obtained. Data reproducibility was found to be within 2 percent. The estimated uncertainties in the velocity statistics determined from these data sets (consisting of 5,000 measurements each) and from initial system calibration data are as follows:

$$U = \pm 1\% \qquad V = \pm 1.5\%$$

$$u' = \pm 2\% \qquad v' = \pm 2.5\%$$

$$u'v' = \pm 5\%$$

where U and V are the mean axial and radial velocities, u' and v' are the rms of the velocity fluctuations, and u'v' is the correlation between the axial and radial velocity fluctuations.

1.4 Raman Scattering System

The data were extended to include simultaneous measurements of two velocity components and species concentration by combining the two-color LDV system with a Raman scattering system (Dibble et al. 1984). Information on important turbulent transport terms used in modeling equations can be obtained from this data. Raman measurements of gas species concentrations were made using a pulsed dye laser (1-J/pulse, 2 μs pulse width, λ=514.5nm, $\Delta\lambda$=0.4 nm). Further details of the Raman scattering system can be found in Dibble et al. 1984. The beam was focused to a 500-μm waist diameter, which was aligned to overlap the LDV measurement volume. The width of the spectrometer entrance slit determined the length of the Raman probe volume (1 mm), while the height of the probe volume was determined by the laser beam diameter. The vibrational Raman scattered light from C_3H_8 was separated from the collected light with a 3/4-m grating spectrometer and measured on a photomultiplier tube at the exit plane of the spectrometer. At each

spatial location a minimum of 2500 simultaneous pairs of axial and radial velocity and mixture fraction were measured.

The primary sources of error in the Raman scattering measurements are calibration of the light collection system, shot noise, and background fluorescence (primarily from the windows where the laser beam enters and exits the test section). Calibration of the Raman system was done in mixtures of C_3H_8 and N_2. As a measure of the overall efficiency of the collection system 6,000 photoelectrons per Joule of laser light were collected from N_2 in room air. The background fluorescence contribution to the Raman signal was measured by scanning the spectrometer away from the Raman line and determined to be less than 0.5% of the Raman signal from N_2 at STP.

1.5 Data Consistency Checks

Several checks on the data were performed to assess the accuracy of the measurements. Conservation of propane (on a mass basis) was verified by integrating the velocity and the propane mass fraction measurements across the flowfield. The integrations were carried out at three axial locations(x/D=15, 30, and 50) and the total propane mass flux was compared with the calibrated value based on the mass flow meter reading. The total propane mass flux at the jet exit was 2.3 gm/sec, and the mass flux calculated at each axial location agreed with this value within 5 percent. In addition to the conservation of propane, momentum must also be conserved across the flowfield. Integration of the total momentum at the above three axial locations was found to agree within 3 percent of the inlet value.

2. Inlet Conditions

Radial profiles of the mean and rms fluctuating axial velocity were measured in the coflowing air stream at the test section inlet (x/D=0) using hot-wire anemometry and are shown in Fig. 1. Radial distance, y, is normalized by the jet exit diameter, D. The growth of a thin boundary layer with a thickness of approximately 0.3 jet diameters is apparent along the outer edge of the jet tube. At increasing radial distances the mean and fluctuating velocity rapidly approach free stream values of 9.2 m/s and 0.4 percent, respectively. As noted previously, the velocity profiles at the fuel tube exit are consistent with fully-developed turbulent pipe flow.

Scattered laser light from the jet tube required that Rayleigh scattering measurements of propane mixture fraction be made downstream of the jet exit where scattered light was sufficiently reduced. Shown in Fig. 2 are the mean and fluctuating propane mixture fraction at an axial distance of 4 diameters downstream of the jet exit. The mean mixture fraction values of unity (corresponding to pure propane) indicate the existence of a potential core, which extends approximately 0.2 diameters from the centerline.

The corresponding mean axial and radial velocity profiles at x/D=4 are shown in Fig. 3. Note that in the sign convention adopted, positive and negative values of radial location, y, simply refer to the right and left sides of centerline, respectively. Results are shown for the case of LDV seed particles added to the coflowing air only and to the jet fluid only and are thus conditional on fluid originating from the coflowing air and from the central fuel jet. The maximum value of mean axial velocity at the centerline ($u_{j,max}$ = 69 m/s) is consistent with fully-developed pipe flow theory ($u_{cl}/u_{j,bulk}$ = 1.28). The mean radial velocity profiles indicate rapid entrainment of coflowing air (negative values of v_{air} to the right of centerline) and rapid outward expansion of fluid originating from the jet (positive values of v_{jet} to the right of centerline). Radial profiles of the axial and radial velocity component (rms) fluctuations, u' and v', and their correlation, u'v', are also shown.

3. Experimental Data Description

Selected mixture fraction and velocity data are presented and briefly discussed. Included in the discussion are axial and radial profiles, probability distributions, and joint probability distributions of propane mixture fraction and velocity.

3.1 Mixture Fraction

The centerline variations in the mean and fluctuating mixture fraction are shown in Fig. 4. The rms of the mixture fraction fluctuations, f', is normalized by the mixture fraction at the centerline, f_{cl}. The mean mixture fraction, f, remains nearly constant over the potential core region, which extends approximately 4 jet diameters downstream of the jet exit, before decreasing rapidly as coflowing air is entrained by the high velocity jet and mixes with the propane. After the initial core region, the fluctuations increase rapidly downstream of the jet exit. In the downstream region, the fluctuations continue to increase but at a slower rate.

The jet spreading rate can be determined from the mean mixture fraction profiles and is characterized by the mixture-fraction half radius, L_f, defined as the radial location at which the mixture fraction is equal to half its value at the centerline. The variation in L_f (normalized by the jet exit diameter) with axial distance is shown in Fig. 5. Note that the virtual origin for the mixture fraction half radius, $x_0/D = -1$, has been subtracted from the axial distance.

Variations in f and f' are shown in Fig. 6 as a function of radial distance normalized by the jet diameter, D. Results are presented for values of x/D=4, 15, 30 and 50. Also shown are the radial variations in the intermittency, γ, which is defined as the fraction of time that the mixture fraction is greater than a near-zero threshold (a value of zero corresponding to pure air). Typical probability density distributions in the mixing region consist of an intermittency spike associated with unmixed air and a broader distribution corresponding to mixed air and propane. The finite width of the intermittency spike requires the somewhat arbitrary selection of a threshold value to differentiate between unmixed and mixed fluid. The threshold value of mixture fraction used was $f_{th} = 0.015$. At all axial locations, a region exists near the centerline for which γ is unity, indicating that turbulent mixing is insufficient to transport unmixed air into the central region. Radial variations in the third and fourth moments of the mixture fraction (skewness, S, and kurtosis, K, respectively) are shown for x/D=15, 30 and 50 and can be compared with the values of S and K for a Gaussian distribution of zero and 3.0, respectively. At the centerline the skewness has a slightly negative value (S=-0.4) and the kurtosis is 3.5.

Probability density distributions of the mixture fraction p(f) were calculated from 8,000 measurements at each spatial location using 50 bins equally spaced over the 3-sigma limits of the data. Radial variations in p(f) are shown in Fig. 7 for x/D=30. Near the centerline the distributions are dominated by a broad Gaussian-like distribution corresponding to a turbulent mixture of propane and entrained air while at outer radial locations a sharp spike corresponding to pure air at f=0 is observed.

3.2 Velocity

The centerline variation in mean axial velocity, U, and the fluctuating components of axial and radial velocity, u' and v', are shown in Fig. 8. The mean axial velocity remains nearly constant for approximately 2 jet diameters downstream of the jet exit, before decreasing rapidly to approach the outer coflowing air velocity of 9.2 m/s farther downstream. Both the axial and radial velocity

fluctuations increase rapidly to a maximum at about x/D=10 before decreasing slowly with downstream distance.

Radial profiles of the mean and fluctuating axial and radial velocities and their correlation, u'v', are shown in Fig. 9 for an axial location of x/D=15. The solid line indicates data collected when seed particles are added to the fuel jet only; the dashed line indicates data collected with only the coflowing air stream seeded. A large difference exists between the conditional radial velocities v_{air} and v_{jet}. Both v_{air} and v_{jet} indicate net outward flow of fluid away from the centerline. The axial velocity fluctuations u'_{jet} and u'_{air} are nearly the same at the centerline. Both u'_{jet} and u'_{air} have a maximum in the mixing region between the fuel jet and the coflowing air where the gradient of the mean velocities is largest. The radial velocity fluctuations v'_{jet} and v'_{air} show a trend that is analogous to the radial profiles of axial velocity components. Both fluctuating components are comparable at the centerline and both decrease with increasing radii. The correlations between the axial and radial velocity fluctuations, $u'v'_{jet}$ and $u'v'_{air}$, show only slight differences near the centerline and increase at large radial distances. Similar trends are seen in the radial profiles at x/D=30 (Fig. 10) and x/D=50 (Fig. 11)

Probability density distributions of the axial velocity conditional on the jet fluid $p(u)_{jet}$ and on the air $p(u)_{air}$ are shown in Fig. 12 for x/D=30 at various distances from the centerline. The distributions were calculated from 3,000 velocity measurements at each spatial location using 30 bins equally spaced over the 3-sigma limits of the data. The solid line indicates data conditional on the air and the dotted line indicates data conditional on the jet fluid. The radial velocity distributions $p(v)_{air}$ and $p(v)_{jet}$ at x/D=30 are shown in Fig. 13.

4. Previous Model Results

This flow has been modeled previously with the intent of assessing both the model and the trends in the data. The results thus represent a benchmark against which other models can be compared. A detailed description of the model and comparisons with the data can be found in Gouldin et al. (1986). Briefly, the model is a second order closure model. The model consists of transport equations for mean velocity, mixture fraction, Reynolds stress components, variance of mixture fraction, scalar fluxes, kinetic energy and scalar dissipation. The results showed reasonably good agreement with experimental trends and the magnitude of the velocity and mixture fraction statistics.

5. Data Filenames and File formats

The Rayleigh data is available as an axial profile along the centerline and radial profiles at x/D=4, 15, 30, and 50. In the format adopted the first two columns give the axial and radial locations x/D and y/D, respectively. The remaining columns give the mean density and propane mixture fraction, the rms of the fluctuations of density and mixture fraction, the intermittency, and the third and fourth moments. Comment lines at the top of each table give descriptive information on the filename, the flow conditions and the type of profile presented. The corresponding probability density distributions of the mixture fraction along the centerline and at each radial location for x/D=15, 30 and 50 are also tabulated. Two columns are given for each location, the mixture fraction f and the probability P (f) corresponding to that mixture fraction. All pdf's were calculated for 50 bins equally spaced over the 3 standard deviation limits of the data.

The velocity data files are presented in a similar format. These files contain a centerline profile and radial profiles at x/D=4, 15, 30, and 50. Axial and radial locations are again located in the first two columns. In addition to the mean axial and radial velocities, U and V, the rms of each velocity

component, and the correlation of u and v are given. At each location two sets of data are tabulated, the first corresponding to results with only the coflowing air seeded with LDV particles and the second corresponding to LDV seed added to the propane jet. The pdf's of axial and radial velocity are tabulated at locations along the centerline and at selected radial locations for x/D=15, 30 and 50. At each location the pdf of the axial velocity p(u) is located in columns 1 and 2 and the pdf of the radial velocity p(v) in columns 3 and 4. Again two data sets are given at each location corresponding to whether the measurements were made with LDV seed added to the coflowing air or the propane jet.

The file names were selected to convey information about the type of data contained (velocity or mixture fraction) and the location. For all data files the first character is "P", indicating propane jet. The next two characters indicate axial centerline profile ("AX") or axial location of a radial profile ("04" for example corresponds to x/D=4). For the Rayleigh data the extension .RAY indicates statistical density and mixture fraction data, while .PDF indicates probability density distribution data. For the velocity data, the extensions .AIR and .JET indicate statistical data conditional on LDV seed added to the coflow air or the propane jet, respectively, while .PDF is probability density distribution data. In the .PDF files for the velocity data, a "J" or "A" in the fourth character position indicates seed added to the propane jet or the coflowing air, respectively.

The complete tabulated data set is stored in the archive SANDC3H8.JET. The directory structure for the archive is as follows:

SANDC3H8.JET - main directory

vel - subdirectory of velocity data
velstat - subdirectory with .JET and .AIR files containing statistical velocity data
velpdf - subdirectory with .PDF files containing probability density distributions of velocity data

ray - subdirectory of density and mixture fraction data
raystat - subdirectory with .RAY files containing statistical density and mixture fraction data
raypdf - subdirectory with .PDF files containing probability density distributions of mixture fraction data

All data files are ASCII text files containing a description header and columns of data with columns separated by one or more spaces.

6. References

Dibble, R. W., Kollmann, W., and Schefer, R. W., "Conserved Scalar Fluxes Measured in a Turbulent Nonpremixed Flame by Combined Laser Doppler Velocimetry and Laser Raman Scattering," Combust. Flame **55**, pp. 307-321 (1984).

Dibble, R. W., Kollmann, W. and Schefer, R. W., "Scalar Dissipation in Turbulent Reacting Flows: Measurements and Numerical Model Predictions, " Twentieth Symposium (International) on Combustion, The Combustion Institute, Pittsburgh, 1985.

Dibble, R. W., Hartmann, V., Schefer, R. W. and Kollmann, W., "Conditional Sampling of Velocity and Scalars in Turbulent Flames using Simultaneous LDV-Raman Scattering," Exper. Fluids **5**, pp. 103-113 (1987).

Gouldin, F. C., Schefer, R. W., Johnston, S. C. and Kollmann, W., “Nonreacting Turbulent Mixing Flows”, Prog. Energy Combust. Sci. **12**, pp. 257-303 (1986).

Johnston, S. C., Dibble, R. W., Schefer, R. W., Ashurst, W. T. and Kollmann, W., “Laser Measurements and Stochastic Simulations of Turbulent Reacting Flows,” AIAA J. **24**, pp. 918-937 (1986).

Schefer, R. W., Johnston, S. C., Dibble, R. W., Gouldin, F. C. and Kollmann, W., "Nonreacting Turbulent Mixing Flows: A Literature Survey and Data Base", Sandia Report SAND86-8217, Sandia National Laboratories, Livermore, CA, 1985.

Schefer, R. W. and Dibble, R. W., "Rayleigh Scattering Measurements of Mixture Fraction in a Turbulent Nonreacting Propane Jet," Paper No. AIAA-86-0278, presented at AIAA 24th Aerospace Sciences Meeting, Reno, NV, January 6-9, 1986.

Schefer, R. W., Hartmann, V. and Dibble, R. W., "Conditional Sampling of Velocity in a Turbulent Nonpremixed Propane Jet," Sandia Report SAND87-8610, February, 1987.

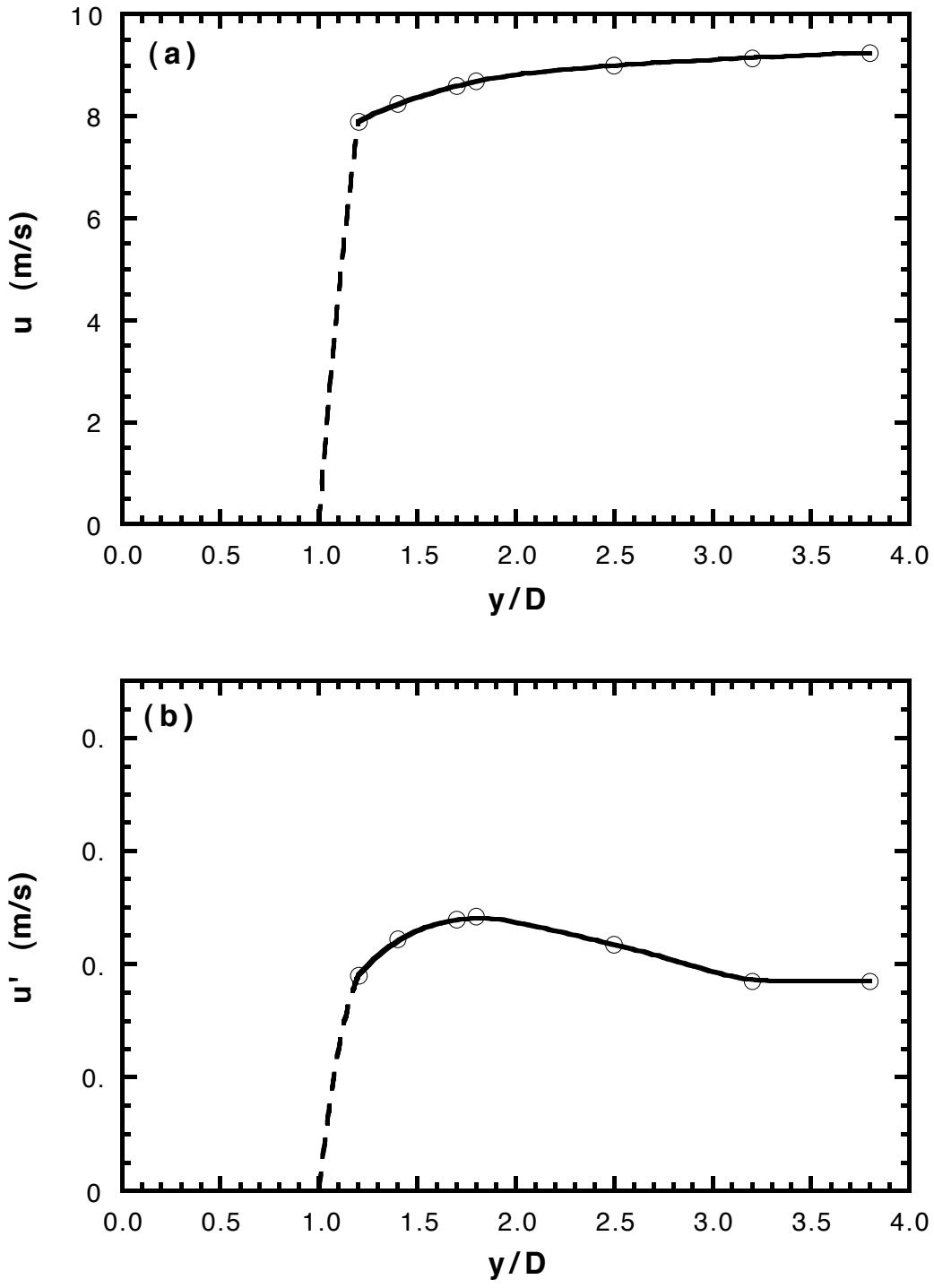

Fig. 1. Inlet profiles of mean and fluctuating axial velocity. (a) Mean axial velocity; (b) axial velocity rms fluctuations

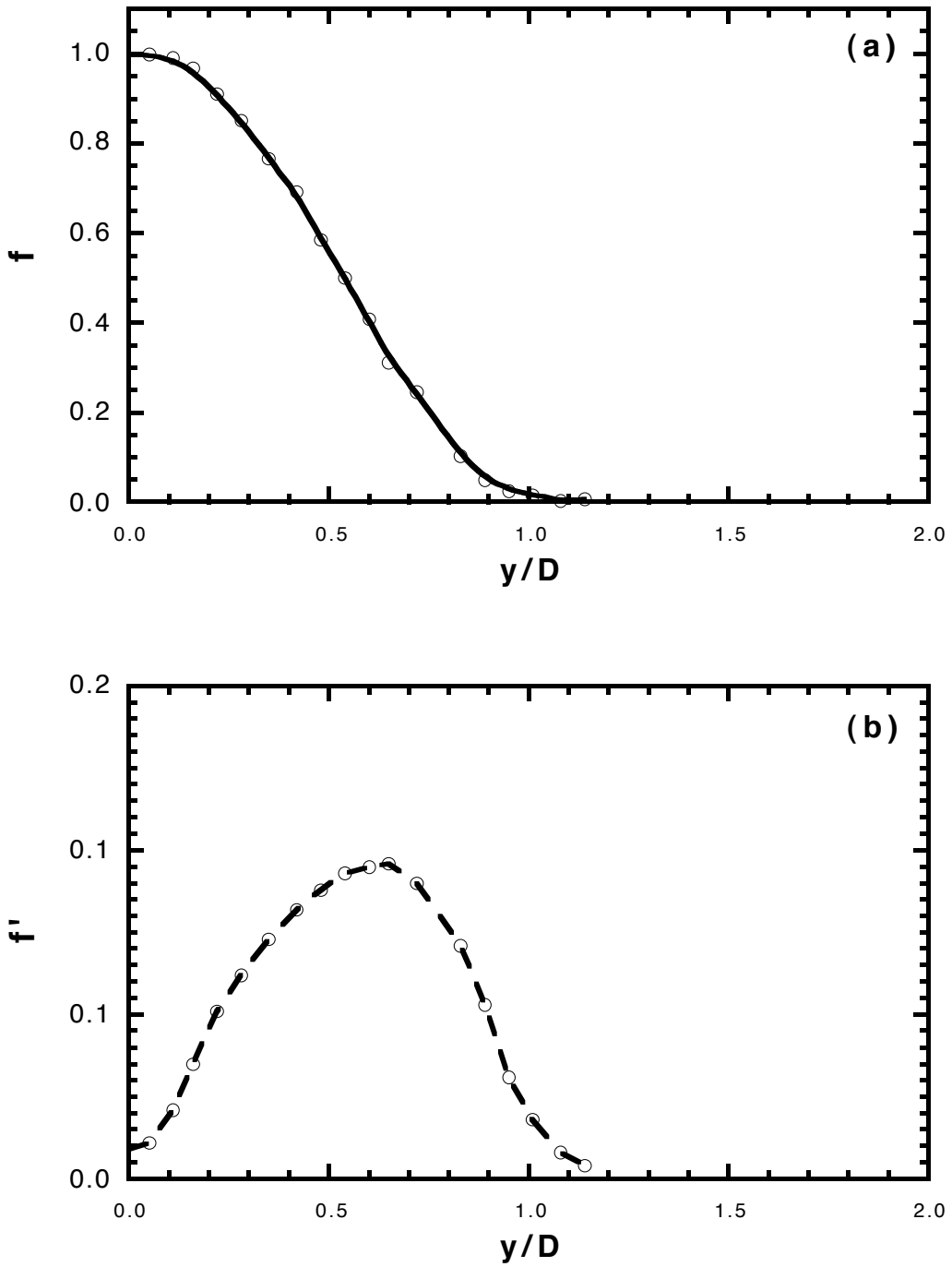

Fig. 2. Radial profiles of mean and fluctuating mixture fraction at x/D=4. (a) Mean mixture fraction; (b) mixture fraction rms fluctuations.

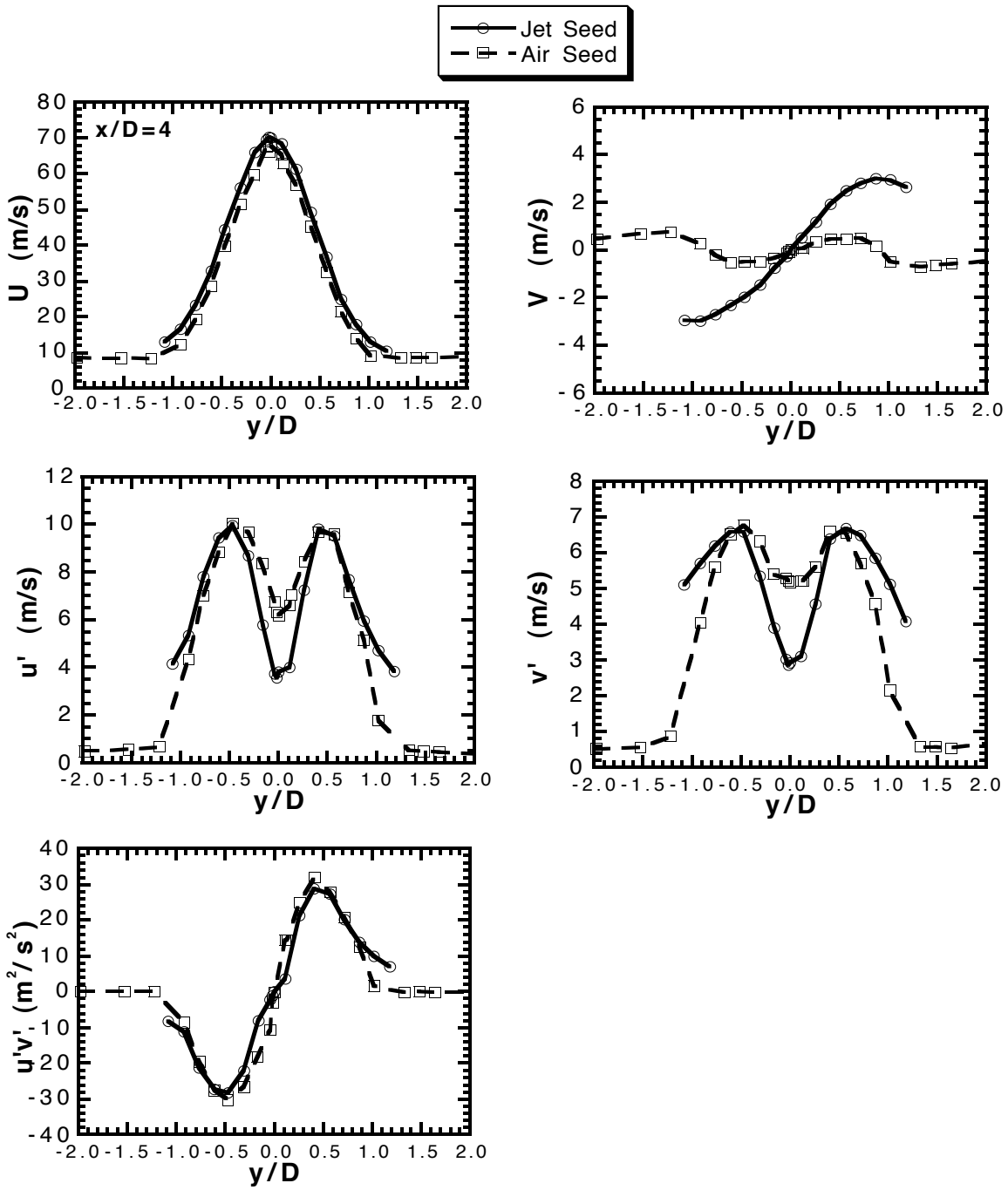

Fig. 3. Radial profiles of mean axial and radial velocity, axial and radial component fluctuations, and their correlation at x/D=4.

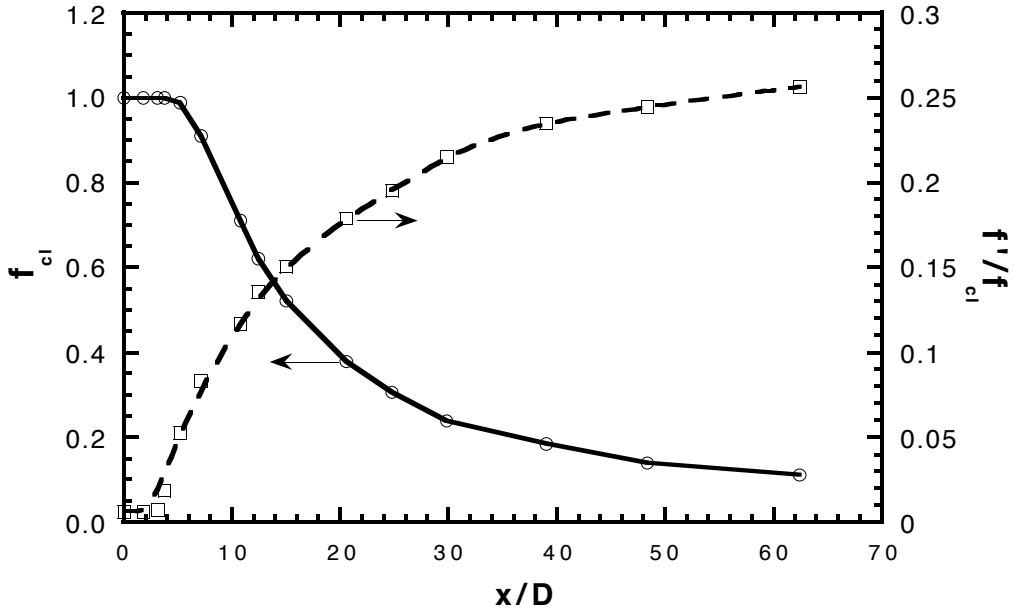

Fig. 4. Centerline profiles of mean mixture fraction and mixture fraction fluctuations.

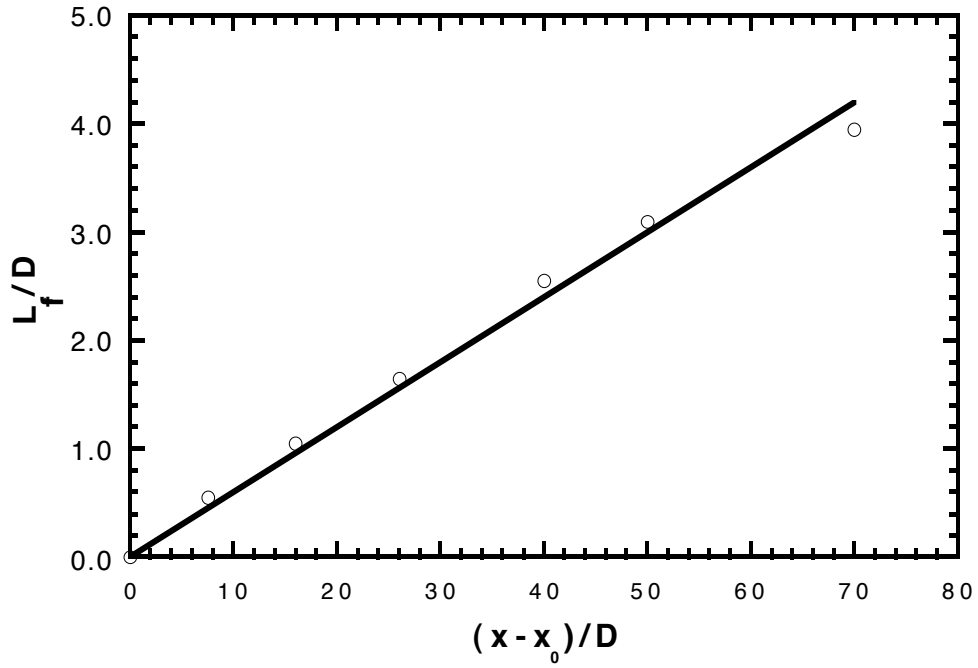

Fig. 5. Variation of mixture fraction half radius with axial distance.

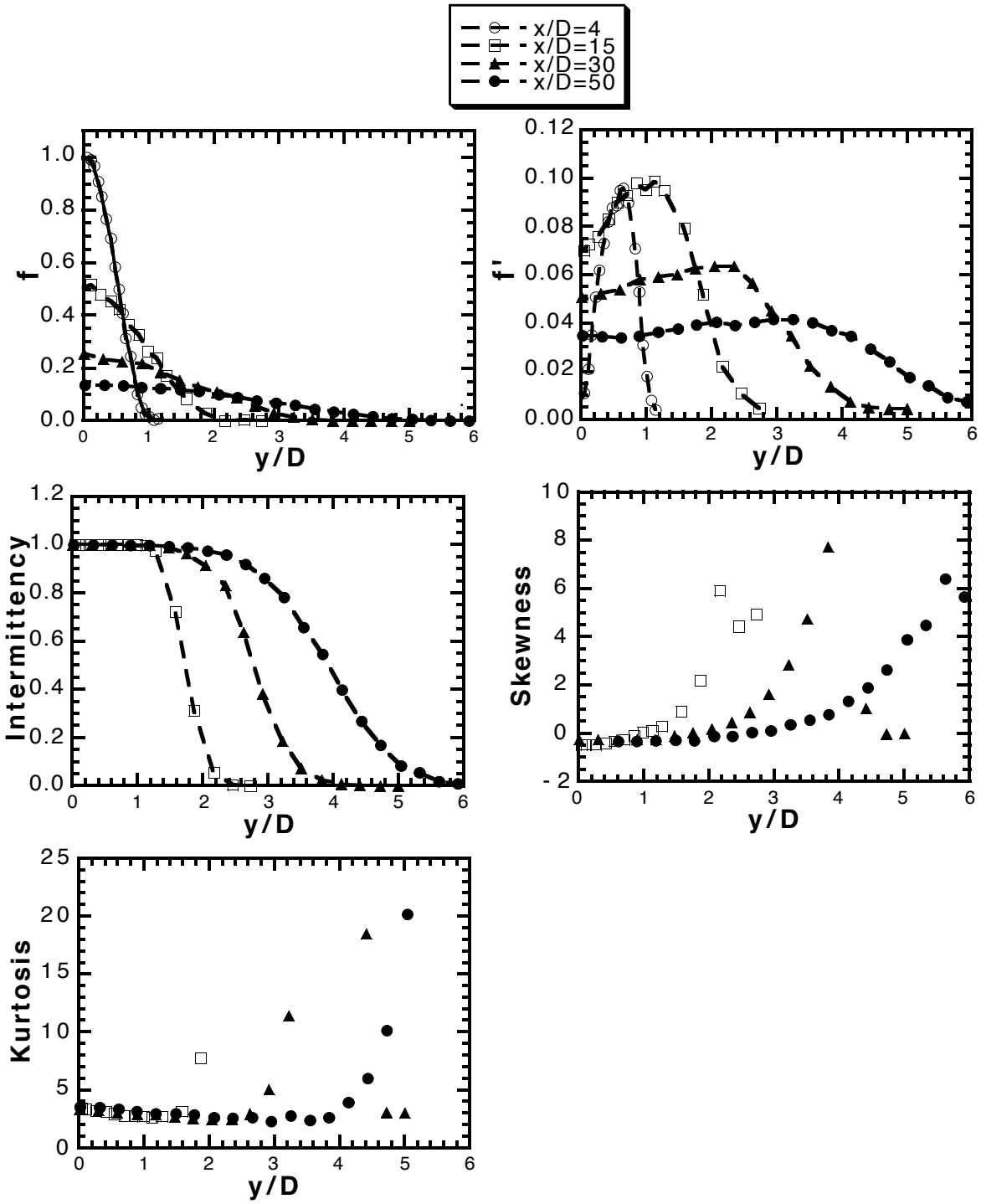

Fig. 6. Radial profiles of mean mixture fraction, mixture fraction fluctuations, intermittency, skewness and kurtosis at x/D=4, 15, 30 and 50.

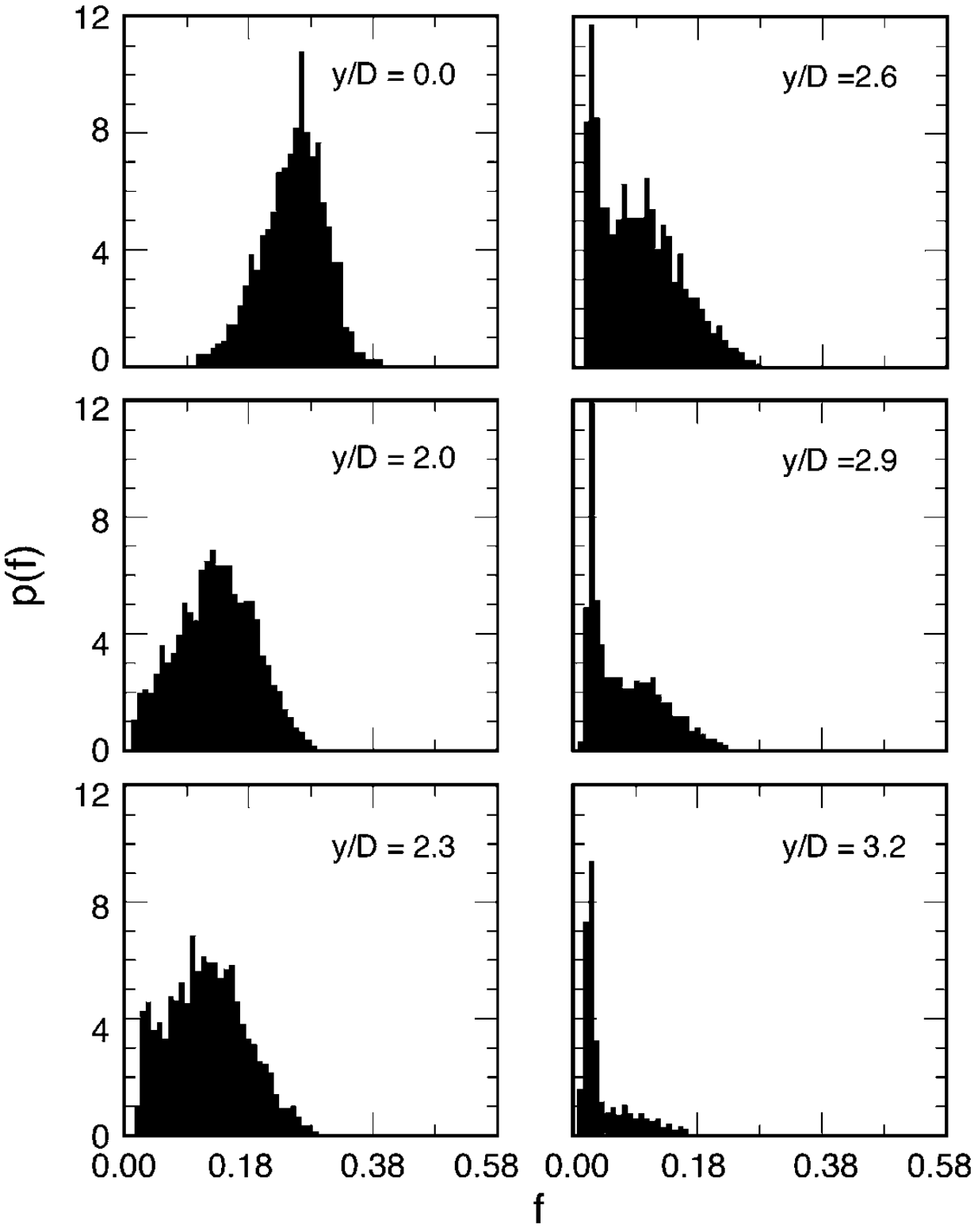

Fig. 7. Probability density distributions of mixture fraction at x/D=30.

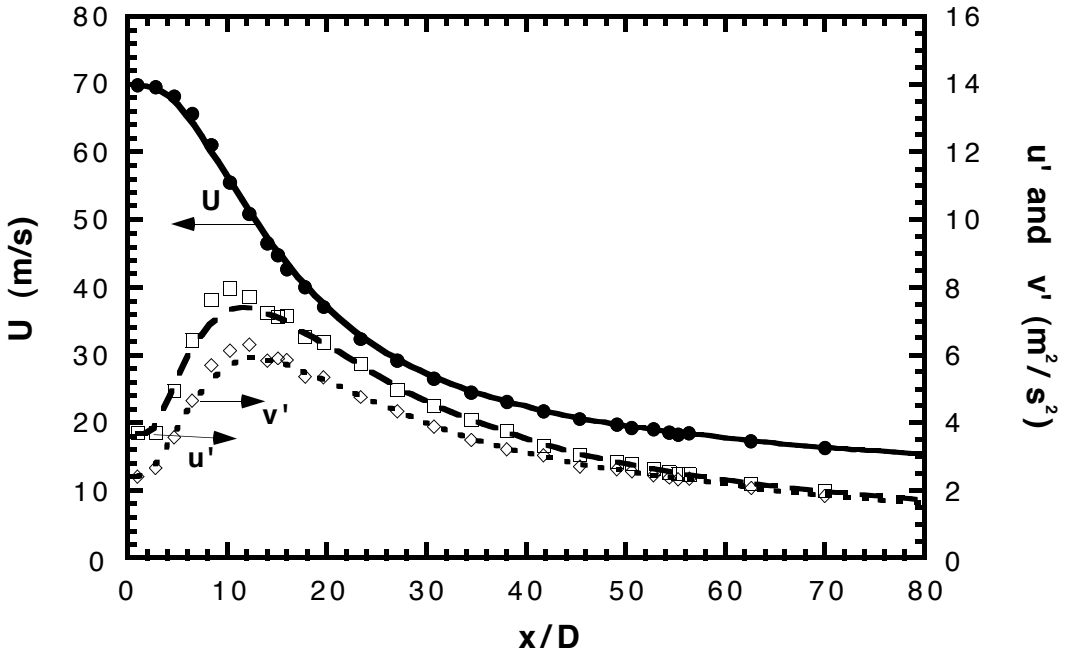

Fig. 8. Centerline profiles of mean axial velocity and axial and radial component fluctuations.

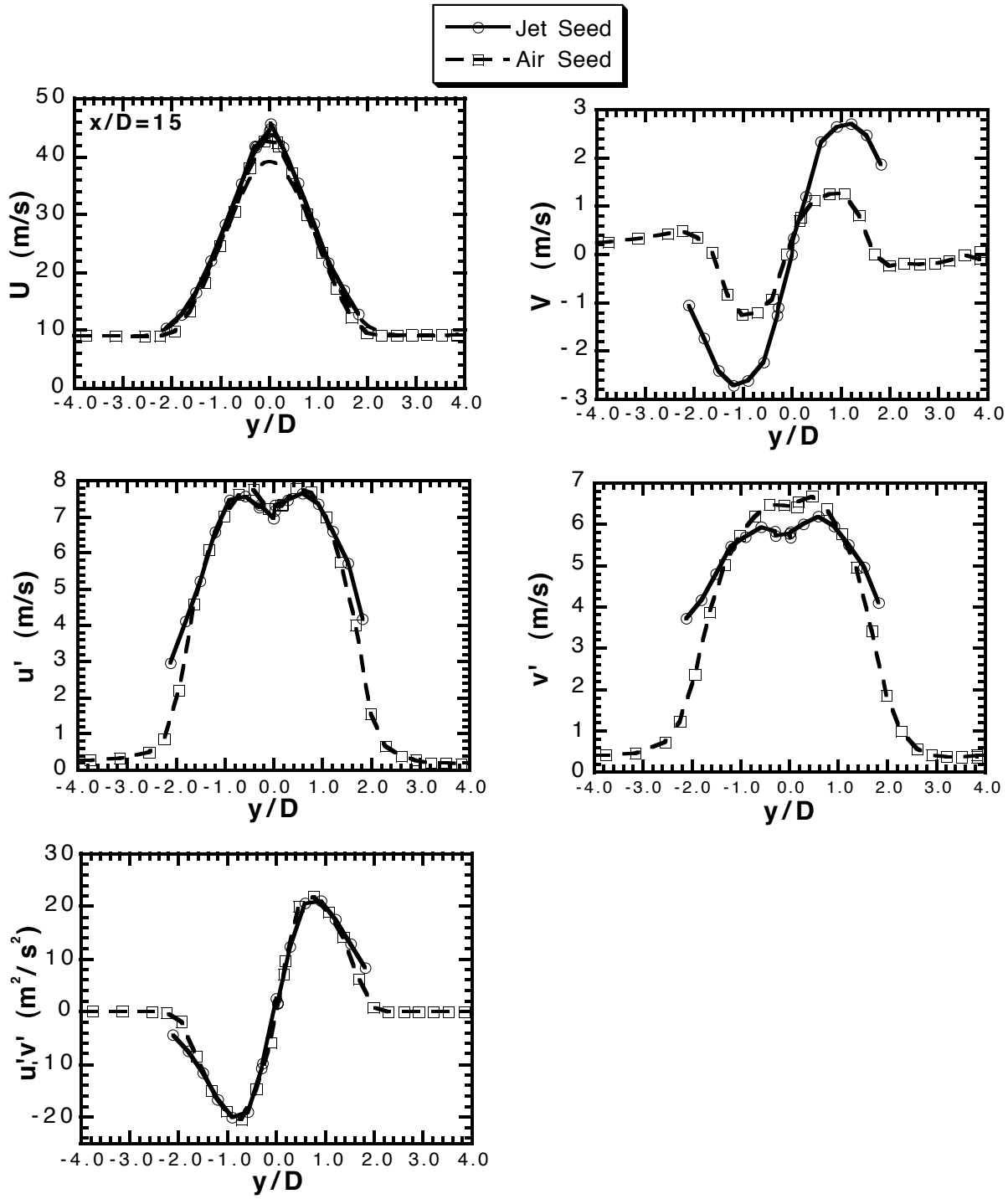

Fig. 9. Radial profiles of mean axial and radial velocity, axial and radial component fluctuations, and their correlation at x/D=15.

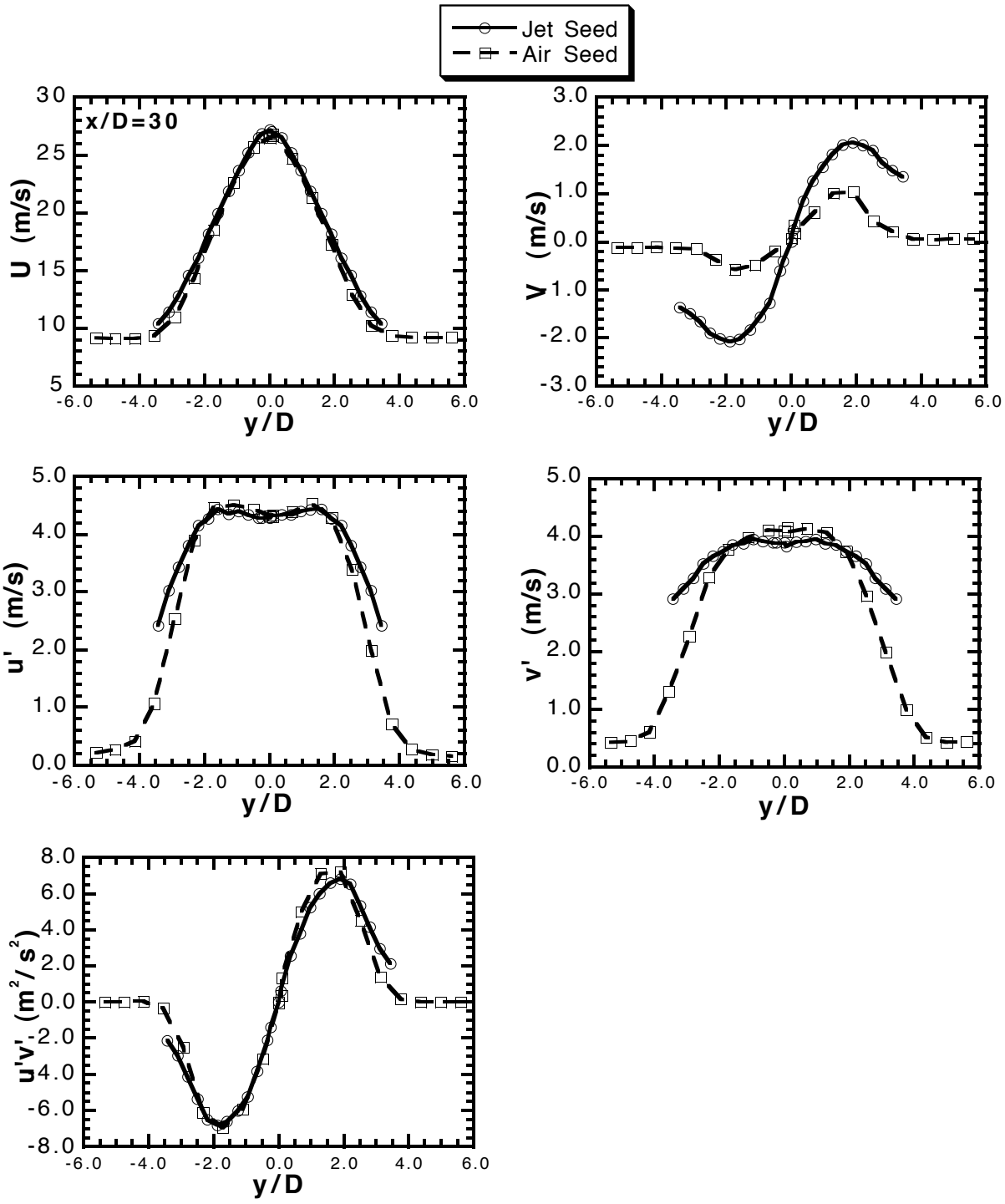

Fig. 10. Radial profiles of mean axial and radial velocity, axial and radial component fluctuations, and their correlation at x/D=30.

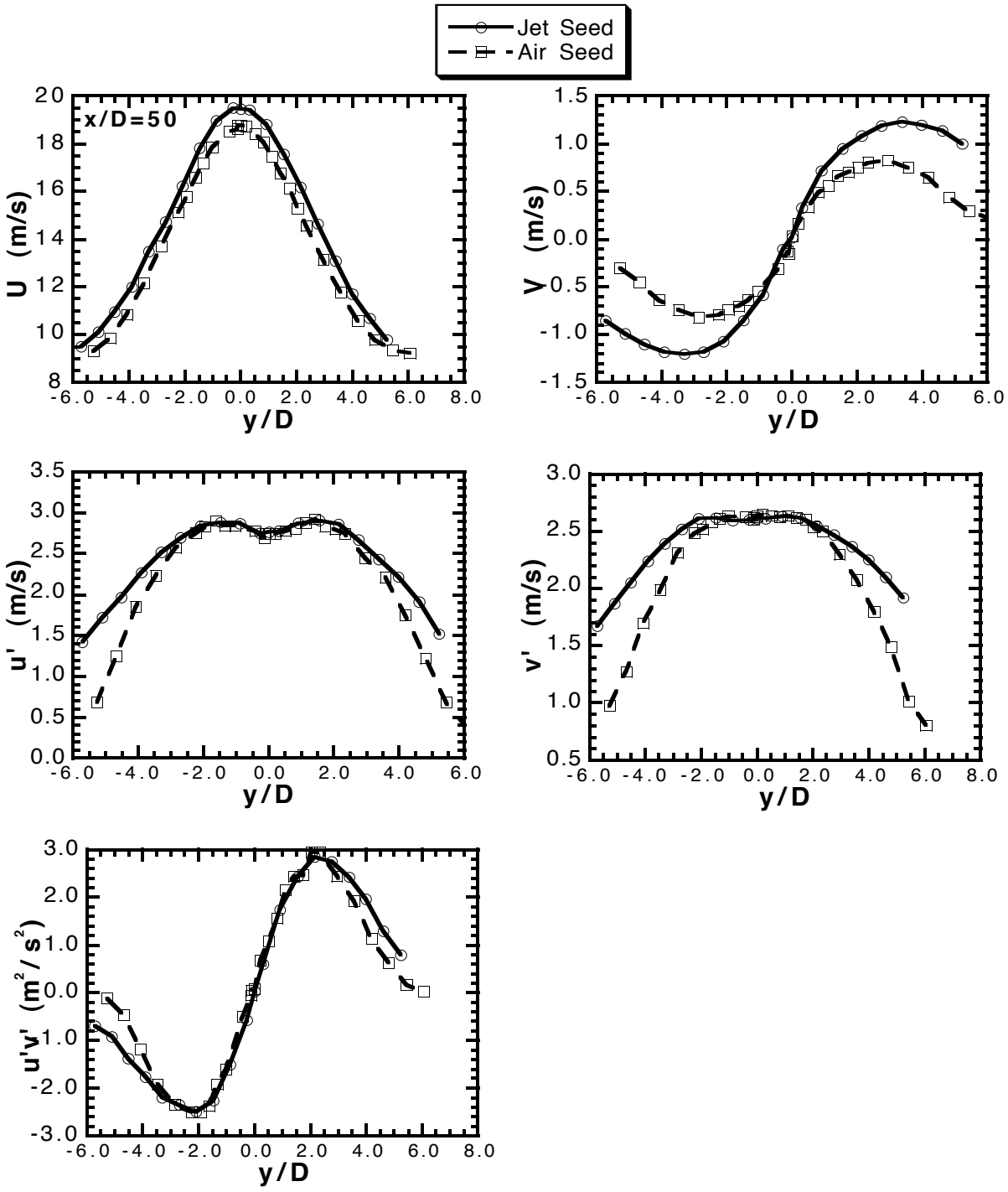

Fig. 11. Radial profiles of mean axial and radial velocity, axial and radial component fluctuations, and their correlation at x/D=50.

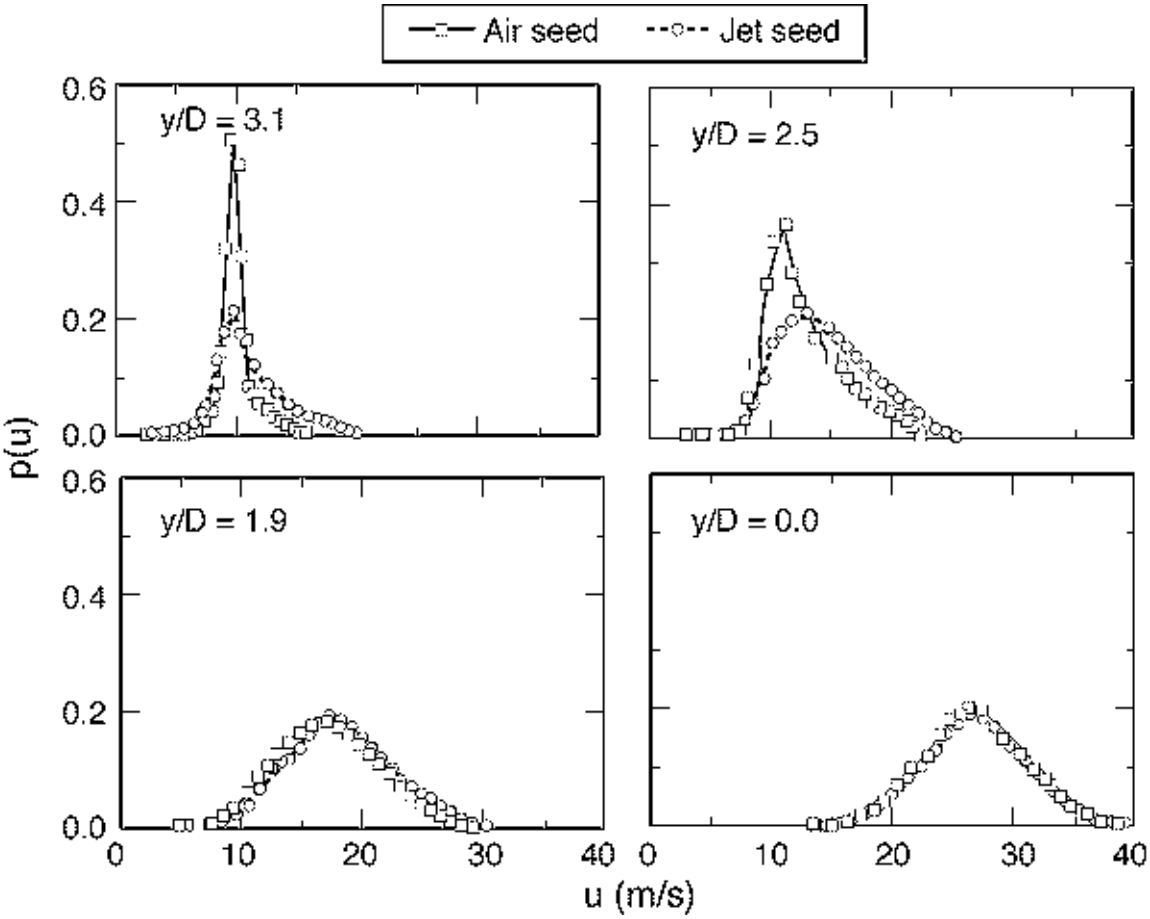

Fig. 12. Conditionally sampled probability density distributions of axial velocity at an axial location of x/D=30.

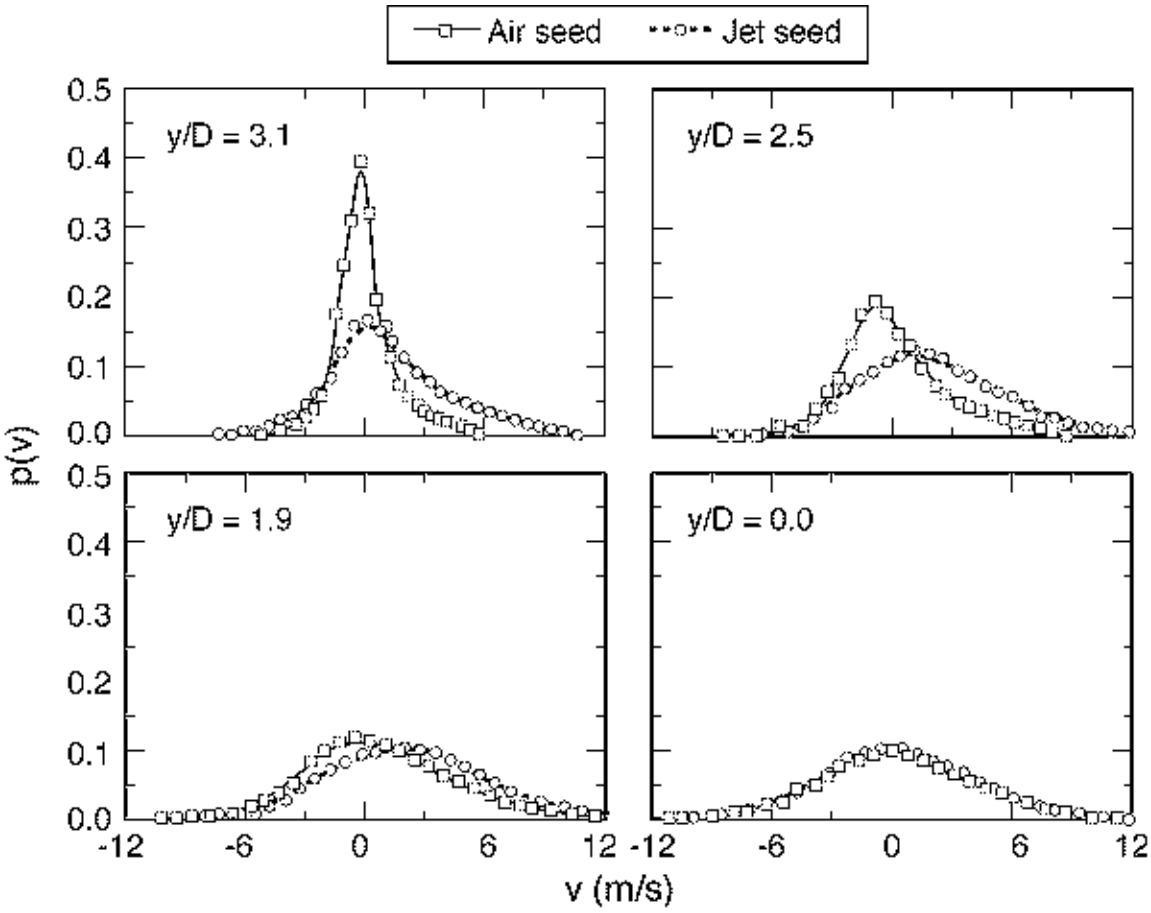

Fig. 13. Conditionally sampled probability density distributions of radial velocity at an axial location of x/D=30.